Sensors & Transducers, Vol. 259, Issue 5, October 2022, pp. 45-51

www.sensorsportal.com

Sensors & Transducers

Published by IFSA Publishing, S. L., 2022
http://www.sensorsportal.com

Measurement Site Selection and Validation in Extracorporeal Circuit for Predictive Maintenance of Blood Coagulation using Photoacoustic Imaging of LED Light Source

[1] Takahiro Wabe, [2,3] Ryo Suzuki, [4] Akimitsu Fujii, [5] Yohsuke Uchida, [2,3] Kazuo Maruyama and [1] Yasutaka Uchida

[1] Teikyo University of Science, Department of Life & Health Sciences, Faculty of Life & Environmental Sciences, 2-2-1 Senjyusakuragi, Adachi-ku, Tokyo, Japan
[2] Faculty of Pharma-Science, Teikyo University, 2-11-1 Kaga, Itabashi-ku, Tokyo, Japan
[3] Advanced Comprehensive Research Organization (ACRO),Teikyo University, 2-21-1 Kaga, Itabashi-ku, Tokyo, Japan
[4] Tokyo college of Medico-Pharmaco Technology, 2-11-1 Higashikasai, Edogawa-ku, Tokyo, Japan
[5] Shuto iko, 1-7-3 Nishisinjuku, Sinnjuku-ku, Tokyo, Japan
Tel.: + 8169101010, fax: + 8169103800
E-mail: takahiro091@gmail.com

Received: 5 September 2022 /Accepted: 7 October 2022 /Published: 31 October 2022

Abstract: Blood purification therapy that removes pathogenic substances and unnecessary blood components in blood is performed by extracorporeal circulation therapy that draws blood out of the body. In extracorporeal circulation therapy, blood is filled in the circuit and circulated outside the body by a pump, but the blood coagulates due to a foreign body reaction in the circuit. Anticoagulants such as heparin are used as blood coagulation measures, but they are not absolute. There is a need for a measurement method that can be predicted before blood coagulation. Photoacoustic imaging was used for predictive maintenance measurements. In photoacoustic imaging used for extracorporeal circulation therapy, the amount of data used must be reduced because it is constantly measured. Accordingly, in this study, we identified areas where photoacoustic imaging changes significantly over time due to blood coagulation, and reduced the volume of data by limiting the area to be measured to 233 pixels where 218240 pixels are normally required for measurement. In addition, because we were able to identify the measurement site, based on that, we develop a predictive maintenance system based on changes in blood coagulation over time in an extracorporeal blood circulation circuit that simulates the environment of extracorporeal blood circulation therapy.

Keywords: Blood coagulation, Photoacoustic imaging, LED, Extracorporeal circulation therapy, Predictive maintenance.

1. Introduction

Blood purification therapy is a treatment method that removes toxic substances and unnecessary blood components that cause diseases accumulated in the blood. Hemodialysis is a typical example, and it covers a wide range of areas such as apheresis and blood cell adsorption therapy [1-3]. The blood

purification therapy introduced here is a treatment method that utilizes extracorporeal circulation. Blood purification therapy uses a pump to pump blood out of the body to provide treatment tailored to each symptom. Blood drawn out of the body for treatment causes blood coagulation when it comes into contact with an artificial foreign substance in the circuit. When blood coagulation occurs, it causes blood clots, so it is customary to stop blood purification therapy when signs appear and then replace it with a new extracorporeal circulation circuit. Since the signs of blood coagulation cannot be detected in advance with a margin, the medical staff involved in the treatment is forced to take immediate action, which puts a heavy load on them. In addition, when replacing the extracorporeal circulation circuit, there is a problem that the patient's blood must be discarded together with the circuit. As a measure against blood coagulation that causes these problems, an anticoagulant typified by heparin is generally used [4-7]. However, anticoagulants are not absolute and it is difficult to completely prevent blood coagulation during extracorporeal circulation therapy. As a safety measure, blood coagulation is detected using a pressure sensor in the extracorporeal circulation circuit. The pressure sensor reacts ex post facto only after the circuit is clogged by blood coagulation or when the viscosity of the blood becomes extremely high and the pressure rises. Therefore, a highly sensitive measurement method (predictive maintenance) that can observe changes in the state of blood coagulation in extracorporeal circulation therapy in advance is required. Therefore, we proposed photoacoustic imaging as a new measurement method that continuously captures the progress of blood coagulation in the circuit and leads to predictive maintenance. The principle of photoacoustic imaging is as follows. The object to be measured irradiated with light energy causes volume expansion due to heat and generates elastic waves (photoacoustic waves). Photoacoustic waves are received and imaged by an ultrasonic probe. Photoacoustic imaging is a promising imaging technology for a wide range of biomedical applications with the potential for high contrast and high spatial resolution. By applying diagnostic imaging to photoacoustic imaging, blood coagulation in the extracorporeal circulation circuit we thought that predictive and conservative measurement was possible. In addition, since it is assumed that the measurement will be performed by photoacoustic imaging in the hospital, an LED light source was used as the light source instead of the laser light source used for conventional photoacoustic imaging. In the previous paper, we reported the basic experimental results showing the possibility of blood coagulation measurement by small photoacoustic imaging of measuring instruments [8-13]. When the photoacoustic imaging image is analyzed using the capacity as it is from the image obtained by the above measurement, the amount of data is large and the processing is burdensome. Therefore, instead of measuring the entire extracorporeal circulation circuit, we thought that we could try to reduce the volume of data within the range that does not affect predictive maintenance by identifying the sites where changes are significant before and after blood coagulation. In addition, the selection of the measurement target site will lead to the miniaturization of the light source and acoustic probe in the future. In selecting the measurement target site, the threshold value of the change in brightness over time, which is a feature amount for the photoacoustic imaging measurement data, was analyzed and examined using MATLAB.

In addition, using MATLAB (Diagnostic Feature Designer), we explore the possibility of developing a predictive maintenance system based on changes in blood coagulation over time in an extracorporeal blood circulation circuit that simulates the environment of extracorporeal blood circulation therapy.

2. Method

2.1. Photoacustic Imaging of the Air Trap Chamber (Bmode)

For the photoacoustic imaging device, AcousticX (CYBERDYNE, INC.), which uses an LED as a light source, was used. As a preliminary experiment, as a result of measuring the extracorporeal circulation circuit by photoacoustic imaging, the reaction of the air trap chamber was the strongest, and almost no reaction was seen in other parts. Therefore, the measurement site was further narrowed down using the air trap chamber as the measurement target. At the time of measurement, an extracorporeal circulatory device and circuit actually used in the medical field were used to flow blood. Fig. 1 shows a schematic diagram of the experimental equipment used in this study.

In addition, a transparent gel spacer (CYBERDYNE, INC.) With an acoustic impedance equivalent to that in water was directly sandwiched between the LED light source and the ultrasonic probe for measurement. The transparent gel spacer does not affect the application of light energy.

As shown in Fig. 1, two high-intensity high-speed pulse-driven LED light source arrays were attached to both sides of the ultrasonic probe using a jig. The angle was about 40°. The distance between the ultrasonic probe and the air trap chamber via the transparent gel spacer was about 1 cm. The LED array used a wavelength of 850 nm, and the light energy was about 200 μJ / pulse, the pulse width was 70 ns, and the repetition frequency was 4 kHz. An ultrasonic probe with a center frequency of 7 MHz was used. The addition average was performed 64 times.

When conducting blood purification therapy for extracorporeal circulation, a large amount of blood is used. It costs money to use a large amount of blood, and it takes time and money to dispose of it after the experiment. In the early stages of research, it is

difficult to use large amounts of blood within the budget, so we decided to use cheap, commercially available blood (sheep blood) that does not affect the reproducibility of blood coagulation in the circuit. The details of the sheep blood used are as follows. It is shown in Table 1.

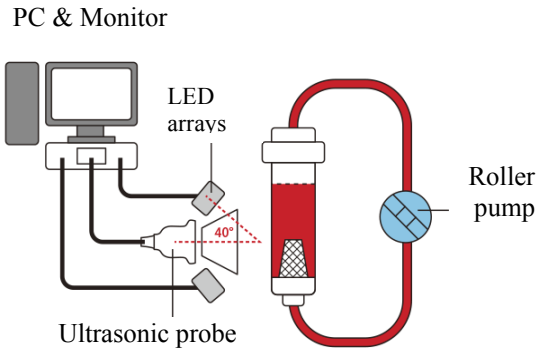

Fig. 1. Configuration diagram of the experiment.

Table 1. Blood used.

Aseptic storage blood of sheep	100ml/container
KOHJIN BIO	No.12070210
Anticoagulant	Alsever liquid

The commercially available blood used is anticoagulated with the anticoagulant ALSEVER'S SOLUTION for transport. Of course, blood does not coagulate as it is, so calcium, which is a coagulation factor, is required to promote blood coagulation. This time, we used calcium gluconate as a coagulation promoter. The upper limit solubility of calcium gluconate is 3.3 g per 100 ml. 1.1 g of calcium gluconate dissolved in 33 ml of saline was injected into 50 ml of blood to promote blood coagulation.

2.2. Selection of Measurement Points

ImageJ, a free software, was used to analyze the luminance of the B-mode image (grayscale image) obtained in Section 2.1, and MATLAB was used to extract the feature amount, and the change in luminance due to blood coagulation was analyzed.

For the input image, 4 × 4 pixels were set as one cell, and 1 × 10 cells were set as one block. Each time the analysis sites using ImageJ, an image processing software, were analyzed so as to overlap each other, the luminance distribution was investigated by shifting them one block at a time in the vertical direction. In the horizontal direction, 4 × 4 pixels were set as one cell. The analysis was performed in the range of 1 × 10 cells as one block. Fig. 2 shows the relative positional relationship between the allocated block numbers and the air trap chamber.

The brightness 126 - 173 used in the measurement was measured in the vertical and horizontal directions of the air trap chamber based on the experimental results reported previously. Vertical and horizontal measurements are described later in Tables 2 and 3, respectively. Based on these results, sites where the photoacoustic wave changes significantly before and after blood coagulation in the extracorporeal blood circulation circuit were identified. In order to show the relative positional relationship between the air trap chamber and the measurement site, the measurement results in Tables 3 and 4 were superimposed on the diagram of the air trap chamber to form Fig. 2.

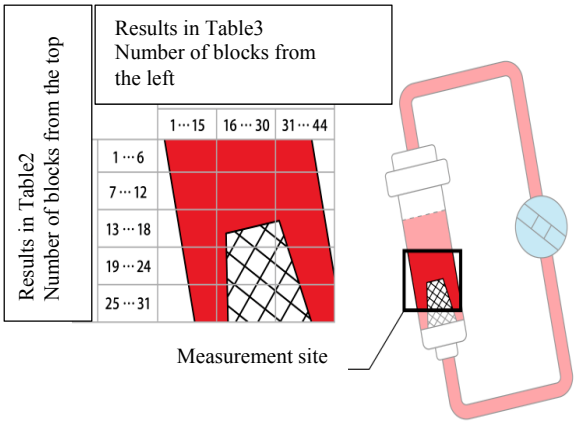

Fig. 2. Relative view of measurement results and air trap chamber.

2.3. Prototype of Predictive Maintenance Program for Changes in Blood Coagulation Over Time in the Extracorporeal Blood Circulation Circuit

Measurements were performed 11 times each at (a) 0 minutes after calcium gluconate injection, (b) 2 minutes, (c) 5 minutes, and (d) 10 minutes. The measurement results had to be biaxial for the convenience of analysis in MATLAB. Therefore, the luminance range was divided into two, 126 - 149 and 150 - 173. The number of cells showing brightness levels of 126 - 149 and 150 - 173 at the measurement site was counted. Furthermore, the time to blood coagulation was expressed as (a) Long, (b) Medium (c) Short, and the state of blood coagulation. In addition, 10 minutes after calcium gluconate injection, blood coagulation is completed, so it was defined as (d) Urgent. The measurement results are shown in Table 2.

Table 2. Measurement result by photoacoustic imaging to the selected luminance range and measurement site.

		Luminance		condition
		126～149	150～173	
min.	1	288	32	Long
	2	306	43	Long
0	3	397	2	Long
	4	424	0	Long
	5	437	0	Long
	6	423	0	Long
	7	432	0	Long
	8	431	0	Long
	9	459	0	Long
	10	482	0	Long
	11	512	0	Long
2	1	170	84	Medium
	2	174	81	Medium
	3	205	87	Medium
	4	237	78	Medium
	5	241	95	Medium
	6	283	96	Medium
	7	283	105	Medium
	8	328	81	Medium
	9	318	89	Medium
	10	330	80	Medium
	11	330	85	Medium
5	1	260	81	Short
	2	215	102	Short
	3	208	101	Short
	4	175	115	Short
	5	161	71	Short
	6	131	86	Short
	7	135	84	Short
	8	137	84	Short
	9	134	94	Short
	10	165	114	Short
	11	198	106	Short
10	1	311	56	Urgent
	2	304	60	Urgent
	3	308	62	Urgent
	4	288	69	Urgent
	5	288	63	Urgent
	6	292	59	Urgent
	7	260	77	Urgent
	8	238	71	Urgent
	9	223	65	Urgent
	10	227	57	Urgent
	11	212	67	Urgent

Since the number of measurements was small, we explored the temporal changes in blood coagulation in the extracorporeal blood circulation circuit by classification learning in order to explore the possibility of regression (supervised learning). Analysis results by MATLAB are shown in Fig. 3. The vertical axis represents the number of cells showing luminance levels 126-149 within the measurement range, and the horizontal axis represents the number of cells showing luminance levels 150-173. The blood coagulation states shown in Table 2 are expressed as (a) Long: blue, (b) Medium: red, (c) Short: yellow, and (d) Urgent: purple. In addition, ○: Correct and ×: False are ○: Correct if they match the prediction model created from the existing data in Table 2, and ×: False if they do not match. Since the number of measurements was small, cross-validation (5 divisions) was performed to prevent overfitting.

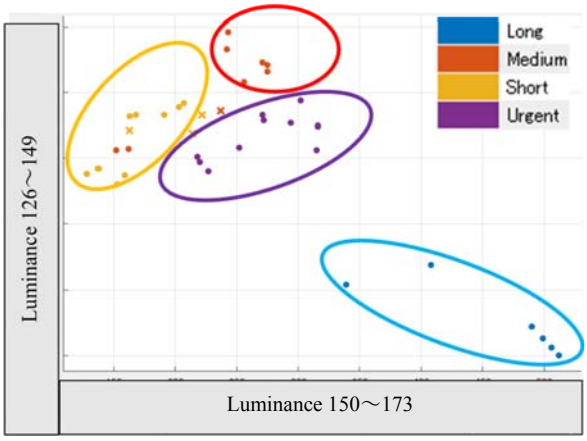

Fig. 3. Results of classification learning with MATLAB.

Long at 0 minutes after injecting calcium gluconate is concentrated in the lower right of the graph, and Medium, Short, and Urgent are gathered in the upper left. It can be seen that the distribution moves counterclockwise from Long as it becomes Urgent.

A suitable algorithm was examined for the data obtained in Tables 2. Fine KNN and fine Gaussian SVM had the highest accuracy at 90.96 %.

As an example, we confirmed the occurrence of prediction correctness for the true value of fine KNN. The confusion matrix obtained from fine KNN is shown in Fig. 4. The vertical line represents the actual class, and the horizontal line represents the predicted class. A mixture matrix is a classification table that expresses the number of measurements and the ratio of correctly predicted Urgent data to those whose actual data is Urgent when evaluating the performance after creating a learning system. It is possible to extract the feature amount of correctness judgment of prediction.

The positive predictive value (PPV) was 100 % for Long and Urgent, 88.9 % for Medium and 76.9 % for Short. The precision of fine KNN is also high, and the bias of prediction from the positive predictive value (PPV) is not high. We believe that a prototype for predictive maintenance could be made under the conditions in this section.

3. Results

3.1. Photoacoustic Imaging (B mode) Results of Air Trap Chamber

Fig. 5 shows the changes over time in blood coagulation that occurred in the air trap chamber using photoacoustic imaging (B mode). The circled area

indicates the wall surface of the air trap chamber, the left side of the wall surface is the transparent gel spacer, and the right side is the blood in the circuit. White streaks like ripples of blood in the circuit are photoacoustic waves due to blood coagulation.

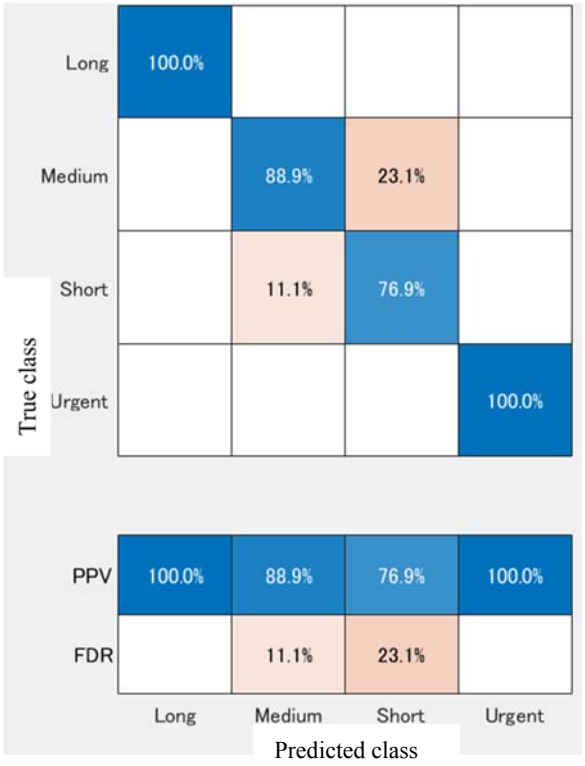

Fig. 4. Confusion matrix obtained from fine KNN.

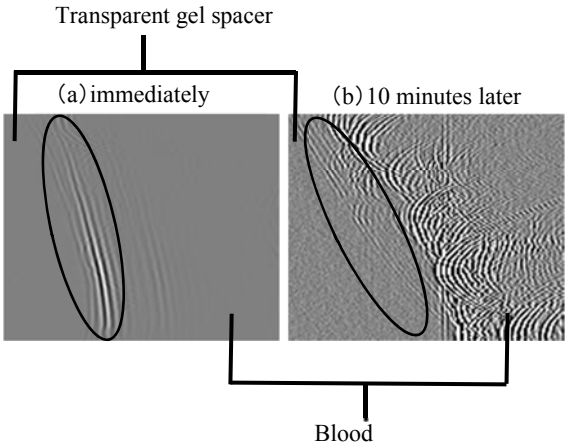

Fig. 5. B mode image by photoacoustic imaging.

3.2. Results of Selection of Measurement Points

The figure (grayscale image) obtained by photoacoustic imaging before and after blood coagulation was subjected to luminance analysis with ImageJ, and the feature quantity was extracted with Rank Features of MATLAB Diagnostic Feature Explorer. Before and after blood coagulation in the extracorporeal circulation circuit, we identified a site where changes in photoacoustic waves were remarkable. Feature extraction was performed by T-test in consideration of increasing the number of measurements in the future. Table 3 shows the measurement results in the vertical direction, and Table 4 shows the measurement results in the horizontal direction.

Table 3. Feature extraction of changes in brightness over time in grayscale images (Vertical direction).

Blocks from the top	T-test	Blocks from the	T-test
1	0.5706	17	0.7727
2	0.6335	18	0.8397
3	0.5937	19	0.7737
4	0.597	20	0.6836
5	0.6816	21	0.6737
6	0.7041	22	0.7307
7	0.7527	23	0.6914
8	0.7233	24	0.7023
9	0.6575	25	0.6722
10	0.7435	26	0.7083
11	0.6734	27	0.7075
12	0.7509	28	0.7581
13	0.6977	29	0.6901
14	0.7829	30	0.6655
15	0.7692	31	0.6762
16	0.8103		

Table 4. Feature extraction of changes in brightness over time in grayscale images (Horizontal direction).

Blocks from the left	T-test	Blocks from the left	T-test
1	0.2867	23	1.4659
2	0.2881	24	1.6364
3	0.2807	25	1.6005
4	0.3019	26	1.5406
5	0.3172	27	1.4555
6	0.3211	28	1.2525
7	0.3567	29	1.2027
8	0.4333	30	1.0604
9	0.4822	31	0.8732
10	0.4895	32	0.8315
11	0.5309	33	0.6781
12	0.6778	34	0.6012
13	0.8276	35	0.6029
14	0.7841	36	0.6345
15	0.7822	37	0.6445
16	0.798	38	0.5969
17	0.5462	39	0.6622
18	0.7156	40	0.6299
19	1.0942	41	0.6708
20	1.5675	42	0.7122
21	1.3059	43	0.6332
22	1.2722	44	0.6036

Table 5 shows a part of the two-dimensional mapping of each component of Table 3 and Table 4. The grayscale image obtained by the measurement was divided into 44 in the horizontal direction and 31 in the vertical direction. The parts showing remarkable changes (0.9 or more) are shown in gray. The shaded areas in the rows and columns are the areas where the T-test changed significantly before and after blood coagulation in the horizontal and vertical directions, respectively. All blocks 19-29 in Table 4 and blocks 13-31 in Table 3 correspond to the mesh filter in the air trap chamber.

From Table 5, it was found that it is possible to measure significant changes over time in photoacoustic waves before and after blood coagulation near and directly above the mesh filter inside the air trap chamber. Blood coagulation appears prominently near the mesh filter because it is a filter that receives blood flow from the front, so it is presumed that the foreign body reaction is stronger than in other parts. It is also possible that blood coagulation (blood clot) generated in other parts of the circuit has peeled off and is caught in the mesh filter. Furthermore, due to the blood flow directly above the mesh filter, blood clots and the like stay and the reaction is thought to be high.

4. Conclusions

In order to realize predictive and conservative measurement of blood coagulation that occurs in the extracorporeal circulation circuit used in the treatment method using extracorporeal circulation represented by blood purification therapy, the previously proposed photoacoustic imaging raises the following problems. (1) The amount of obtained image data is large, and (2) the light source and ultrasonic probe for measurement are large. In order to solve these problems, in this paper, we measured the changes over time in blood coagulation in the extracorporeal circulation circuit, identified the sites where photoacoustic waves were prominent, and selected the measurement sites. From Table 5, by setting the threshold value of 0.9, which is the product of the results of the horizontal and vertical photoacoustic waves, it was possible to select the measurement site where the change is remarkable before and after blood coagulation (gray part). As a result, the measurement range is reduced, and the possibility of reducing the size of the photoacoustic imaging measurement unit (light source, ultrasonic probe) is shown. In addition, when measuring the entire air trap chamber, 218240 pixels are required, but the measurement target site is narrowed down to 233 pixexel to reduce the dose of data by about 1/1000, and the extracorporeal blood circulation circuit using photoacoustic imaging. We were able to reduce the data handled for predictive maintenance of blood coagulation in the body. Therefore, it is considered that the problem of photoacoustic imaging operation for predictive maintenance measurement of blood coagulation occurring in the extracorporeal circulation circuit has been solved.

Machine learning was performed using MATLAB from grayscale images obtained from photoacoustic imaging of the time course of blood coagulation in the extracorporeal blood circulate learning, we made a prototype with supervised learning classification, and found that fine KNN and fine Gaussian SVM were the most accurate prediction models with an accuracy of 90.9 %. From the positive predictive value (PPV) of the mixed matrix, the prediction of Long and Urgent before and after clear blood coagulation was 100 %, with on circuit. In machine the data easily distinguishable, while Medium was 88.9 % and Short was 76.9 %.

Therefore, a predictive maintenance system based on the temporal change of blood coagulation in an extracorporeal circulation circuit simulating the environment of extracorporeal circulation therapy was investigated.

Acknowledgments

T. Wabe and Y. Uchida would like to thank Mr. N. Sato of CYBERDYNE, INC Research and Development Dept, for his cooperation in this experiment.

References

[1]. J. Utley, Pathophysiology of cardiopulmonary bypass: current issues, *J. Card. Surg.*, Vol. 5, Issue 3, 1990, pp. 177-189.

[2]. Y. Mori, Blood compatible material, Kobunshi Ronbunshu, Vol. 42, No. 42, October 1985, pp. 601－615 (in Japanese).

[3]. J. K. Kirklin, A. D. Pacifico, Complement and the damaging effects of cardiopulmonary bypass, *J. Thorac. Cardiovasc. Surg.*, Vol. 86, Issue 6, 1983, pp. 845-857.

[4]. L. Gott, J. D. Whiffen, R. C. Dutton, Heparin bonding on colloidal graphite surfaces, *Science*, Vol. 142, Issue 3597, 1963, pp. 1297-1298.

[5]. I. O. Salyer, Medical Application of Plastic, in Biomedical Material Symposium No. 1, *Interscience*, New York, Vol. 105, 1971.

[6]. M. Murase, A. Usui, M. Maeda, Y. Tomita, F. Murakami, K. Teranishi, T. Koyama, T. Ito, Ot. Abe, Nafamostat mesilate reduces blood loss during open heart surgery, *Circulation*, Vol. 88, Issue 5 Pt2, November 1993, pp. 11432-11436.

[7]. M. Hiroura, A. Usui, M. Kawamura, M. Hibi, K. Yoshida, F. Murakami, J. Iwase, Nafamostat mesilate reduces bloodcell adhesion to cardiopulmonary bypass circuit: an invitro study, *J. Extra Corpor. Technol.*, Vol. 26, Issue 3, September 1994, pp. 121- 125.

[8]. T. Wabe, R. Suzuki, K. Maruyama, Y. Uchida, Possibility for temporal observationof thrombus generated in extracorporeal circulator circuit by photoacoustic imaging using LED, in *Proceedings of the 5th International Conference on Sensors Engineering and Electronics Instrumentation*

Advances (SEIA'19), Canary Islands (Tenerife), Spain, 25-27 September 2019, pp. 157-160.

[9]. T. Wabe, R. Suzuki, K. M*aruyama, Y. Uchida,* The Measurement of Blood Coagulation Process in Extracorporeal Circuit Using LED Photoacoustic Imaging, *Sensors & Transducers*, Vol. 237, Issue 9-10, September-October 2019, pp. 88-94.

[10]. T. Wabe, R. Suzuki, K. Maruyama, Y. Uchida, Possibility for temporal observation of thrombus generated in extracorporeal circulator circuit by photoacoustic imaging using LED, in *Proceedings of the 5th International Conference on Sensors Engineering and Electronics Instrumentation Advances (SEIA' 2019),* Canary Islands (Tenerife). Spain.25-27 September 2019. pp. 157-160.

[11]. T. Wabe, R. Suzuki, K. Maruyama, Y. Uchida, Possibility of Extracting Feature Value from the Changes in Brightness over Time of Blood Coagulation in the Extracorporeal Circuit, *Sensors & Transducers,* Vol. 246, Issue 7, November 2020, pp. 64-70.

[12]. T. Wabe, R. Suzuki, A. Fujii, Y. Uchida, K. Maruyama, Yasutaka Uchida, Basic Research on Blood Coagulation Measurement of Extracorporeal Circulation Circuit Using Photoacoustic Imaging of LED Light Source, *Sensors & Transducers,* Vol. 253, Issue 6, November 2021, pp. 1-8.

[13]. T. Wabe, R. Suzuki, A. Fujii, Y. Uchida, K. Maruyama, Y. Uchida, Selection of measurement site for predictive maintenance of blood coagulation in an extracorporeal circulation circuit using LED photoacoustic imaging and an extracorporeal circulation device, *Proceedings of the 8th International Conference on Sensors Engineering and Electronics Instrumentation Advances (SEIA' 2022)*, 21-23 September 2022, pp. 55-59.

Table 5. Selection of measurement points.

Table3		19	20	21	22	23	24	25	26	27	28	29
Table4	T-test	1.0942	1.5675	1.3059	1.2722	1.4659	1.6364	1.6005	1.5406	1.4555	1.2525	1.2027
1	0.5706	0.624351	0.894416	0.745147	0.725917	0.836443	0.93373	0.913245	0.879066	0.830508	0.714677	0.686261
2	0.6335	0.693176	0.993011	0.827288	0.805939	0.928648	1.036659	1.013917	0.97597	0.922059	0.793459	0.76191
3	0.5937	0.649627	0.930625	0.775313	0.755305	0.870305	0.971531	0.950217	0.914654	0.86413	0.743609	0.714043
4	0.597	0.653237	0.935798	0.779622	0.759503	0.875142	0.976931	0.955499	0.919738	0.868934	0.747743	0.718012
5	0.6816	0.745807	1.068408	0.890101	0.867132	0.999157	1.11537	1.090901	1.050073	0.992069	0.853704	0.81976
6	0.7041	0.770426	1.103677	0.919484	0.895756	1.03214	1.152189	1.126912	1.084736	1.024818	0.881885	0.846821
7	0.7527	0.823604	1.179857	0.982951	0.957585	1.103383	1.231718	1.204696	1.15961	1.095555	0.942757	0.905272
8	0.7233	0.791435	1.133773	0.944557	0.920182	1.060285	1.183608	1.157642	1.114316	1.052763	0.905933	0.869913
9	0.6575	0.719437	1.030631	0.858629	0.836472	0.963829	1.075933	1.052329	1.012945	0.956991	0.823519	0.790775
10	0.7435	0.813538	1.165436	0.970937	0.945881	1.089897	1.216663	1.189972	1.145436	1.082164	0.931234	0.894207
11	0.6734	0.736834	1.055555	0.879393	0.856699	0.987137	1.101952	1.077777	1.03744	0.980134	0.843434	0.809898
12	0.7509	0.821635	1.177036	0.9806	0.955295	1.100744	1.228773	1.201815	1.156837	1.092935	0.940502	0.903107
13	0.6977	0.763423	1.093645	0.911126	0.887614	1.022758	1.141716	1.116669	1.074877	1.015502	0.873869	0.839124
14	0.7829	0.856649	1.227196	1.022389	0.996005	1.147653	1.281138	1.253031	1.206136	1.139511	0.980582	0.941594
15	0.7692	0.841659	1.205721	1.004498	0.978576	1.12757	1.258719	1.231105	1.18503	1.119571	0.963423	0.925117
16	0.8103	0.88663	1.270145	1.058171	1.030864	1.187819	1.325975	1.296885	1.248348	1.179392	1.014901	0.974548
17	0.7727	0.845488	1.211207	1.009069	0.983029	1.132701	1.264446	1.236706	1.190422	1.124665	0.967807	0.929326
18	0.8397	0.9188	1.31623	1.096564	1.068266	1.230916	1.374085	1.34394	1.293642	1.222183	1.051724	1.009907
19	0.7737	0.846583	1.212775	1.010375	0.984301	1.134167	1.266083	1.238307	1.191962	1.12612	0.969059	0.930529
20	0.6836	0.747995	1.071543	0.892713	0.869676	1.002089	1.118643	1.094102	1.053154	0.99498	0.856209	0.822166
21	0.6737	0.737163	1.056025	0.879785	0.857081	0.987577	1.102443	1.078257	1.037902	0.98057	0.843809	0.810259
22	0.7307	0.799532	1.145372	0.954221	0.929597	1.071133	1.195717	1.169485	1.125716	1.063534	0.915202	0.878813
23	0.6914	0.75653	1.08377	0.902899	0.879599	1.013523	1.131407	1.106586	1.065171	1.006333	0.865979	0.831547
24	0.7023	0.768457	1.100855	0.917134	0.893466	1.029502	1.149244	1.124031	1.081963	1.022198	0.879631	0.844656
25	0.6722	0.735521	1.053674	0.877826	0.855173	0.985378	1.099988	1.075856	1.035591	0.978387	0.841931	0.808455
26	0.7083	0.775022	1.11026	0.924969	0.901099	1.038297	1.159062	1.133634	1.091207	1.030931	0.887146	0.851872
27	0.7075	0.774147	1.109006	0.923924	0.900082	1.037124	1.157753	1.132354	1.089975	1.029766	0.886144	0.85091
28	0.7581	0.829513	1.188322	0.990003	0.964455	1.111299	1.240555	1.213339	1.167929	1.103415	0.94952	0.911767
29	0.6901	0.755107	1.081732	0.901202	0.877945	1.011618	1.12928	1.104505	1.063168	1.004441	0.86435	0.829983
30	0.6655	0.72819	1.043171	0.869076	0.846649	0.975556	1.089024	1.065133	1.025269	0.968635	0.833539	0.800397
31	0.6762	0.739898	1.059944	0.88305	0.860262	0.991242	1.106534	1.082258	1.041754	0.984209	0.846941	0.813266